

УДК 535:621.373.8;535:621.375.8

## МОДЕЛИРОВАНИЕ ФЕМТОСЕКУНДНЫХ ИМПУЛЬСОВ В ПОЛУПРОВОДНИКОВОМ ЛАЗЕРЕ ПРИ ПОСТОЯННОМ ТОКЕ НАКАЧКИ МЕТОДОМ FDTD

**В.В. Макаревич, Е.О. Котьяшёв**

*Могилевский государственный университет им. А.А. Кулешова, Могилев*

## FDTD SIMULATION OF FEMTOSECOND PULSES IN SEMICONDUCTOR LASER UNDER DC PUMPING CURRENT

**V.V. Makarevich, Y.O. Katsiashou**

*A.A. Kuleshov Mogilev State University, Mogilev*

Представлены результаты моделирования динамики излучения полупроводникового лазера на базе уравнений Максвелла-Блоха с использованием метода конечных разностей во временной области (FDTD). Для GaAs поверхностно-излучающих лазеров с вертикальным резонатором с длиной волны 628 нм при постоянной токовой накачке обнаружена возможность существования периодической последовательности фемтосекундных импульсов, длительностью ~ 100 фс.

**Ключевые слова:** метод конечных разностей во временной области, полупроводниковый лазер, фемтосекундные импульсы, когерентное взаимодействие.

Simulation results of semiconductor laser dynamics using finite-differences time domain (FDTD) method of solving Maxwell-Bloch equations are presented. The ~ 100 fs pulse train regimes under continuous pumping were found to be possible for GaAs vertical cavity surface emitting lasers in the 628 nm wavelength region.

**Keywords:** finite-difference time domain method, semiconductor laser, femtosecond pulses, coherent interaction.

### Introduction

Over the last decades generation of ultrashort laser pulses has attracted the interest of many scientists due to their different applications in various spheres of human life.

The expensive mode-locked solid-state lasers of complex design are normally used to achieve ultrashort pulses. However, cheaper semiconductor lasers can also be used to generate ultrashort pulses. In general a mode-locked setup is used in ultrashort semiconductor lasers. In [1] the optically pumped InP-based mode-locked vertical external cavity surface emitting laser (VECSEL) with the semiconductor saturable absorber mirror (SESAM) generated 1.7 ps pulses in 1.56 μm wavelength region. In [2] the optically pumped mode-locked semiconductor disk laser with fast saturable absorber was used to achieve 190 fs pulses at ≈ 1045 nm. In [3] 784-fs pulse duration at 1 W of average output power was achieved in optically pumped quantum dot VECSEL with SESAM. In [4] a new type of mode-locked laser with spatially separated gain medium was simulated.

Numerical methods are usually involved to simulate laser behaviour. The finite-difference time domain (FDTD) method was used in [5] and [6]. In [5] Maxwell-Bloch system was solved with the help of an iterative predictor-corrector FDTD method to study self-induced transparency effect. In [6] Maxwell-Bloch system was used to model VECSEL.

In this paper we introduce FDTD modeling of femtosecond pulses in vertical cavity surface-emitting laser (VCSEL) with small cavity lengths under dc pumping current.

### 1 Laser model and parameters

Coherent interaction of radiation with active particles of gain medium is described by a system of Maxwell-Bloch equations:

$$\begin{aligned} \operatorname{rot} \mathbf{H} &= \frac{\partial \mathbf{D}}{\partial t}, \quad \operatorname{rot} \mathbf{E} = -\mu\mu_0 \frac{\partial \mathbf{H}}{\partial t}, \\ \mathbf{D} &= \varepsilon\varepsilon_0 \mathbf{E} + 2n_a \mathbf{d}_{ab} P, \\ \ddot{P} + 2\gamma\dot{P} + \omega_0^2 P &= \frac{\omega_0^2}{\Omega} \frac{1}{\hbar} \mathbf{d}_{ab} \mathbf{E} N, \\ \dot{N} &= -2\Lambda - \gamma_{nr} (N - N_0) - 4 \frac{\Omega}{\hbar\omega_0^2} \mathbf{d}_{ab} \mathbf{E} \dot{P}, \end{aligned} \quad (1.1)$$

where  $\gamma$  – the relaxation frequency of polarization,  $\gamma_{nr}$  – the relaxation frequency of inversion,  $n_a$  – the density of active particles,  $\omega_0$  – the two-level transition frequency,  $N_0$  – the inversion at the thermal equilibrium state,  $N$  – the inversion rate (–1 at totally excited state and 1 at the ground state),  $P$  – the polarization degree of active particles,  $\mathbf{E}$  – the electric field,  $\mathbf{D}$  – the electric displacement field,  $\mathbf{H}$  – the magnetic field,  $\varepsilon_0$  – the vacuum electric permittivity,  $\varepsilon$  – the electric permittivity,  $\mu_0$  – the vacuum magnetic permeability,  $\mu$  – the magnetic permeability,  $\Omega = (\omega_0^2 - \gamma^2)^{1/2}$ ,  $\Lambda$  – the pumping rate,  $\mathbf{d}_{ab}$  – the

electric dipole moment [6]. All symbols in bold represent vector quantities.

A laser active medium consists of a large number of particles with two energy levels. If the external electric field is not strong enough, all the particles behave independently. Otherwise there is cooperative behaviour. Each active particle presents an electric dipole moment  $\mathbf{d}_{ab}$  that interacts with strong electric field of intracavity laser radiation. As a result of the cooperative interaction, a “giant dipole”, consisting of a large number of phased dipole moments of each particle, comes into being, and radiation rate is becoming proportional to square of interacting particles.

The vector system (1.1) was applied to our one dimensional laser model (figure 1.1) with electric field and dipole moments vectors were parallel and perpendicular to the axis of light propagation. Set of equations of one spatial variable and time was solved numerically using auxiliary differential equation (ADE)-FDTD method [7] on equally spaced grid with spatial step  $a = 0.005\lambda$  ( $\lambda$  – the wavelength) and temporal step  $0.5a/c$  ( $c$  – the speed of light in vacuum). Figure 1.1 illustrates the laser model used for calculations. The gain medium of VCSEL occupied the whole space inside the cavity formed by the facets of a planar structure with dielectric permittivity  $\epsilon = 16$ . Electric field values were sampled at point near the right side of medium.

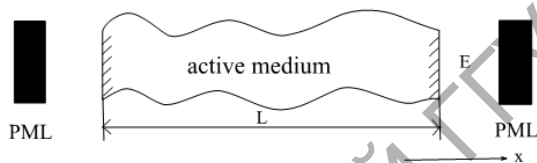


Figure 1.1 – Laser model, used in numerical calculations. PML – perfectly matched layer

The initial conditions were defined as follows. Electric and magnetic fields were set to be zero. Initial incoherent state of medium polarization along spatial coordinate  $x$  was calculated as

$$P(x) = 5 \cdot 10^{-2} \cdot \sin(\omega_0 \cdot x/c + 2\pi \cdot rnd), \quad (1.2)$$

where  $rnd$  is real random value uniformly distributed within  $[0,1]$  range, generated for every space grid point separately.

Random polarization distribution takes some time to establish the state of phased medium dipoles. Therefore the time delay of emergence of laser radiation is higher than in the case of a specific non-random form of polarization distribution. The initial value of medium inversion is equal to 1, which corresponds to the main unexcited state of particles.

There were used invariable parameters of semiconductor GaAs medium:  $\omega_0 = 3 \cdot 10^{15}$  Hz,  $\gamma_{nr} = 3 \cdot 10^8$  Hz,  $\gamma = 1 \cdot 10^{13}$  Hz,  $\mathbf{d}_{ab} = -1.9 \cdot 10^{-29}$  A·s·m,  $N_0 = 1$ ,  $n_a = 5 \cdot 10^{26}$  m<sup>-3</sup>,  $\lambda = 2\pi c/\omega_0 \approx 628$  nm [6, 8].

The lengths of laser active media ranged from  $L = 0.5\lambda$  to  $L = 2.5\lambda$ . Pumping rates ranged from  $\Lambda = 4 \cdot 10^{10}$  s<sup>-1</sup> to  $\Lambda = 9 \cdot 10^{12}$  s<sup>-1</sup>.

## 2 Results and discussion

Three regimes of laser radiation were found during simulation, each of them existed within the subspace of  $L$  (active medium length) and  $\Lambda$  (pumping rate) values. Figure 2.1 shows distribution of all the calculated pairs pumping rate/active media length units. Squares-points depict periodic pulse train regimes (Figure 2.2 (a)). Above the line stars-points depict single frequency regimes (Figure 2.2 (b)), and circle-point depicts frequency beating regime (Figure 2.2 (c)).

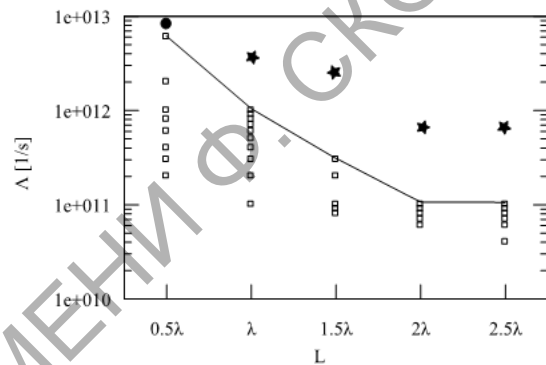


Figure 2.1 – Pumping rate – active medium length diagram

Spectra of the mentioned regimes are represented on figures 2.3 (a), 2.3 (b) and 2.3 (c).

Figure 2.2 (a) shows the time evolution of electric field in the form of a stationary femtosecond pulse train. Pulse duration is 190 fs. Stability of the pulses was observed within temporal interval of calculation, which was 235.6 ps.

The shortest pulses duration of 52 fs were obtained at  $L = 0.5\lambda$  and  $\Lambda = 6 \cdot 10^{12}$  s<sup>-1</sup>.

Some modeling researches were carried out to find out the influence of active medium length and pumping rate on the pulse duration and the pulse repetition time. Figure 2.4 shows rising pulse duration with higher medium lengths, with saturation at  $L > 1.75\lambda$ .

Figures 2.5 (a) and 2.5 (b) illustrate steady decrease of pulse duration value for greater pumping values at two different media lengths.

For fixed lengths of active media, pulse repetition time inversely depends on pumping rate. It is determined by the external pumping rate (Figure 2.6 (a) and 2.6 (b)). In the case when laser cavity is ranged from  $0.5\lambda$  to  $2.5\lambda$ , pulse repetition time does not satisfy the mode-locked equation

$$T = \frac{2L}{c}$$

because numerical values of  $T$  obtained from the equation are less (9 fs – 34 fs) than FDTD calculated ones ( $> 1$  ps).

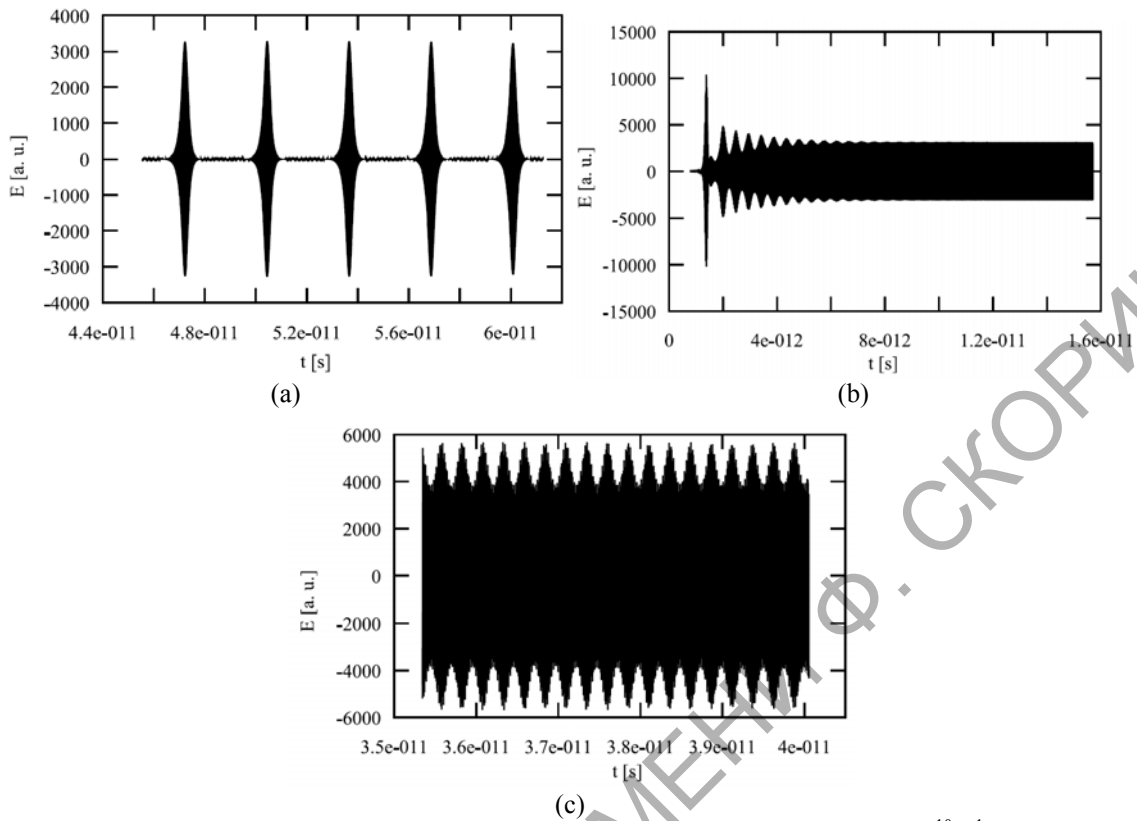


Figure 2.2 – (a) Output electric field versus time at  $L = 2.5\lambda$  and  $\Lambda = 6 \cdot 10^{10} \text{ s}^{-1}$ .  
 (b)  $2.5\lambda$  and  $\Lambda = 8 \cdot 10^{11} \text{ s}^{-1}$ . (c)  $0.5\lambda$  and  $\Lambda = 9 \cdot 10^{12} \text{ s}^{-1}$

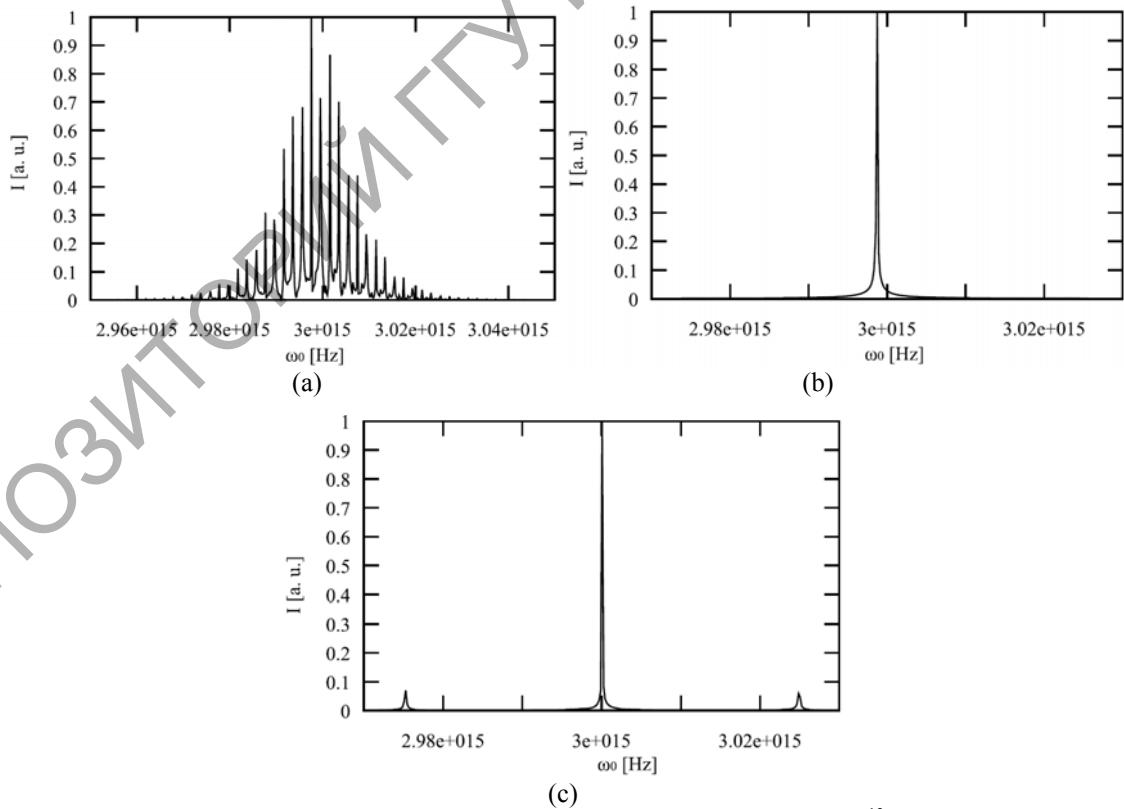


Figure 2.3 – (a) Spectrum of pulse train. Spectral width is  $2 \cdot 10^{13} \text{ Hz}$ .  
 (b) Single frequency spectrum. (c) Triple frequency spectrum

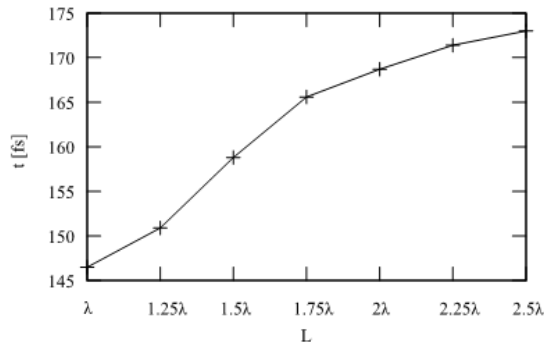


Figure 2.4 – Laser pulse duration versus active medium length at  $\Lambda = 1 \cdot 10^{11} \text{ s}^{-1}$

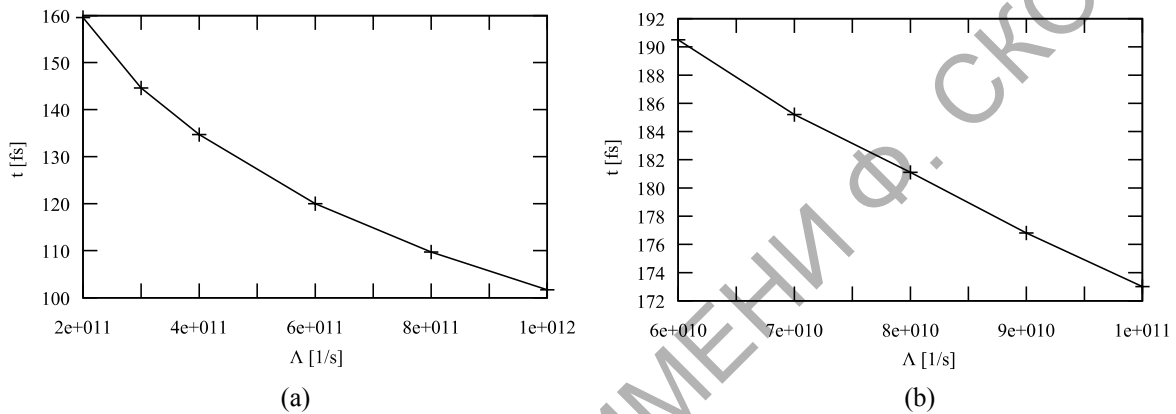


Figure 2.5 – (a) – Laser pulse duration versus pumping rate at  $L = 0.5\lambda$  and (b)  $L = 2.5\lambda$

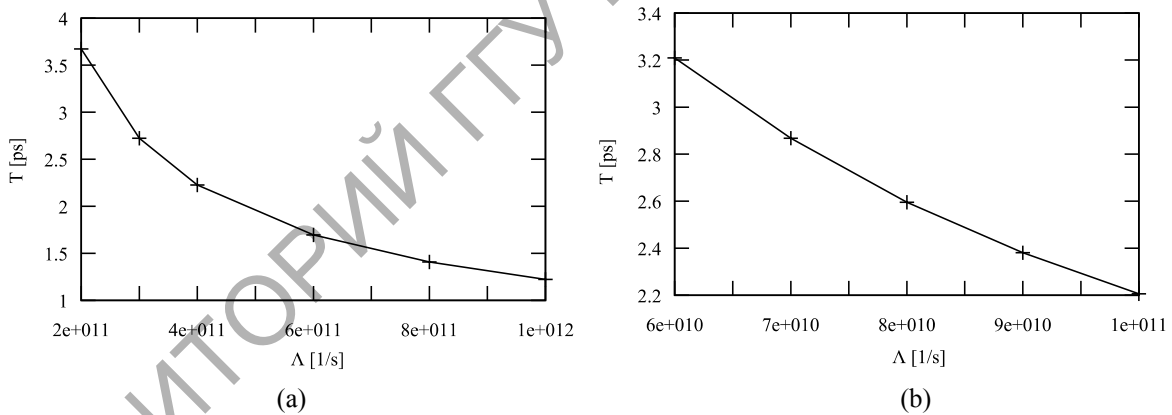


Figure 2.6 – (a) – Pulse repetition time versus pumping rate at  $L = 0.5\lambda$  and (b)  $L = 2.5\lambda$

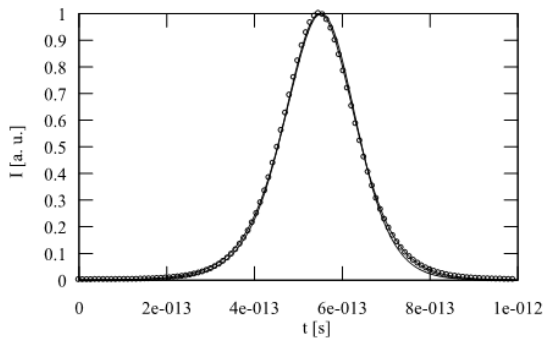


Figure 2.7 – Pulse shape fitting. Solid line indicates the simulated pulse shape, solid line with circles indicates the calculated on (2.1) pulse shape

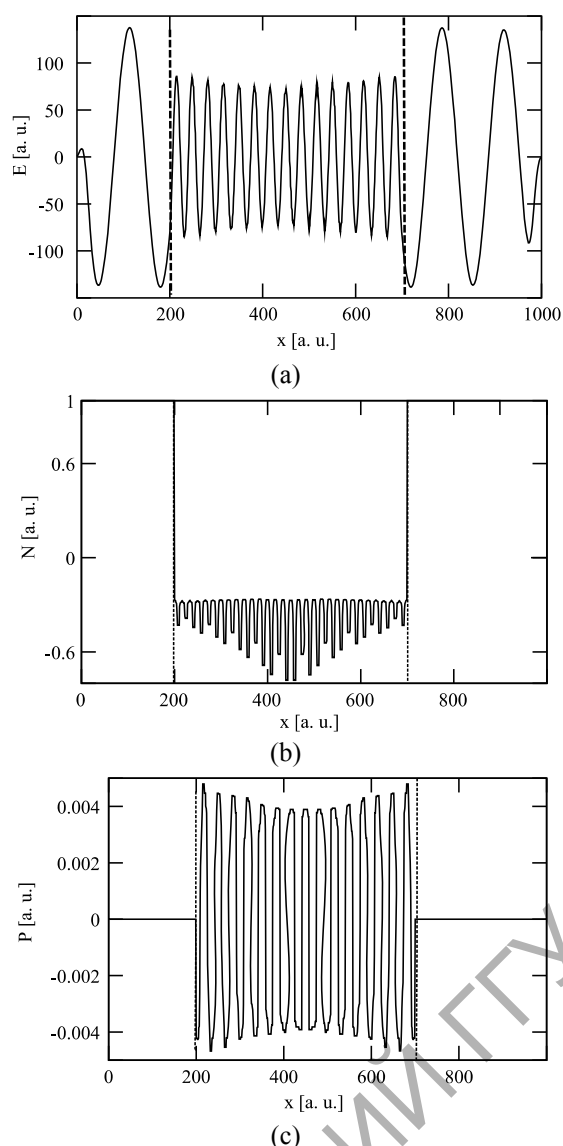


Figure 2.8 – (a) Electric field, (b) inversion and (c) polarization versus coordinate for pulsed regime on figure 2.2 (a). Dashed lines indicate edges of active medium

Laser pulse fitting was performed using equation

$$I = \text{sech}^2[(t - t_0) / \tau], \quad (2.1)$$

where  $\tau$  determines pulse width,  $t_0$  determines initial position of the pulse (Figure 2.7). FDTD simulated intensity envelope of pulse (Figure 2.2 (a)) almost coincides with the one calculated on (2.1).  $\text{sech}^2$ -shaped pulse is a common form of a superfluorescence pulse [9].

Figure 2.8 shows spatial distribution of electric field, inversion and polarization when laser is generating femtosecond pulses. Such deterministic distribution of polarization points at cooperative interaction between active particles of medium and laser radiation.

### Conclusion

Periodic pulsed regime of laser radiation was found as a result of FDTD simulations of VCSEL radiation with pulse durations of 52–190 fs and pulse repetition times of 1.3–3.7 ps. The intensity envelope of an individual pulse has  $\text{sech}^2$  shape. Central wavelength is 628 nm.

This regime has cooperative nature because of well-correlated state of polarization and strongly oscillating inversion.

Our simulations showed the possibility of generation femtosecond pulses from VCSELs under dc pumping current.

Parameters of modeled laser can be used to create femtosecond VCSEL without the passive modulator under dc pumping current.

Pulse repetition time and pulse duration are determined by pumping rate. This can be used in optical networking, signal processing and transmission.

### REFERENCES

1. *Ultrashort pulse generation from 1.56  $\mu\text{m}$  mode-locked VCSEL at room temperature* / A. Khadour [et al.] // Opt. Express. – 2010. – Vol. 18, № 19. – P. 19902–19913.
2. *Mode-locked InGaAs-AlGaAs disk laser generating sub-200-fs pulses, pulse picking and amplification by a tapered diode amplifier* / P. Klopp [et al.] // Opt. Express. – 2009. – Vol. 17, № 13. – P. 10820–10834.
3. *Femtosecond high-power quantum dot vertical external cavity surface emitting laser* / M. Hoffmann [et al.] // Opt. Express. – 2011. – Vol. 19, № 9. – P. 8108–8116.
4. *Modeling of mode locking in a laser with spatially separate gain media* / R.M. Oldenbeuving [et al.] // Opt. Express. – 2010. – Vol. 18, № 22. – P. 22996–23008.
5. *Ultrafast pulse interactions with two-level atoms* / R. W. Ziolkowski [et al.] // Phys. Rev. A. – 1995. – Vol. 52, № 4. – P. 3082–3094.
6. *Klaedtke, A. Spatio-Temporal Non-Linear Dynamics of Lasing in Micro-Cavities. Full Vectorial Maxwell-Bloch FDTD Simulations: Ph. D. thesis* / A. Klaedtke. – Stuttgart, 2004. – 158 p.
7. *Taflove, A. Computational Electrodynamics: The Finite-Difference Time-Domain Method* / A. Taflove. – 2<sup>nd</sup> ed. – Boston, London: Artech House, Inc., 2000 – 852 p.
8. *Васильев, П.П. Роль сильного усиления среды в возникновении сверхизлучения и наблюдении когерентных эффектов в полупроводниковых лазерах* / П.П. Васильев // Квантовая электроника. – 1999. – Т. 29, № 1. – С. 4–8.
9. *Андреев, А.В. Оптическое сверхизлучение: новые идеи и эксперименты* / А.В. Андреев // УФН. – 1990. – Т. 160, № 12. – С. 1–46.

Поступила в редакцию 25.06.12.